Interfacial and volumetric kinetics of the $\beta \rightarrow \delta$ phase transition in the energetic nitramine octahydro-1,3,5,7-tetranitro-1,3,5,7-tetrazocine based on the virtual melting mechanism

Valery I. Levitas[a)]
Center for Mechanochemistry and Synthesis of New Materials, Department of Mechanical Engineering, Texas Tech University, Lubbock, Texas 79409

Laura B. Smilowitz, Bryan F. Henson, and Blaine W. Asay
Los Alamos National Laboratory, Los Alamos, New Mexico 87545

(Received 26 July 2005; accepted 1 November 2005; published online 9 January 2006)

[DOI: 10.1063/1.2140698]

In the recent papers,[1,2] we presented a thermodynamic and kinetic model of the $\beta \rightarrow \delta$ phase transformation (PT) in the organic energetic crystal octahydro-1,3,5,7-tetranitro-1,3,5,7-tetrazocine (HMX). It was based on the hypothesis that the kinetics of the $\beta \rightarrow \delta$ PT is governed by the thermodynamics of melting of the δ phase. In particular, the activation energy for growth was found to be equal to the heat of fusion $\Delta h_{\delta \rightarrow m}$. Nucleation was modeled empirically by the reversible first-order kinetics. The proposed kinetics described the experimental data quite well, however, a number of questions still remain. (1) How does melting govern the solid-solid PT at 432.6 K,[9] a temperature of more than 100 K lower than the melting temperature? (2) The $\beta \rightarrow \delta$ PT is accompanied by a large volumetric expansion, $\varepsilon^t = 0.08$. Thus, the associated energy of internal stresses should be large and should suppress both nucleation and growth. Also the athermal interface friction due to interaction of the interface with the long-range stress field of crystal defects (point defects, dislocations, various boundaries) should suppress the PT. This suppression is observed for other PTs in HMX ($\alpha \leftrightarrow \delta$ and $\alpha \leftrightarrow \beta$ PTs) which produce half the volumetric strain of $\beta \leftrightarrow \delta$ PT and yet occur with significant overheating (overcooling), or in the region of stability of other phases, or are not observed at all.[1–4] Despite this, the $\beta \rightarrow \delta$ PT in Refs. 1 and 2 starts at 432.6 K, just above the phase equilibrium temperature of $\theta_e = 432$ K.[4] (3) Why is the $\beta \rightarrow \delta$ PT accompanied by the nanoscale cracking of the δ phase, considering the compressive stresses in the δ phase? (4) Why are the thermodynamics and kinetics of the first and second $\beta \leftrightarrow \delta$ PTs cycles not affected by the nanocracking? (5) In Ref. 5, experimental data on the β-δ interface velocity are described by an equation with an activation energy equal to $0.42\Delta h_{\delta \rightarrow m}$, which is inconsistent with the mechanism proposed in Refs. 1 and 2. (6) Are the data for interface propagation and overall growth kinetics consistent? Also, we found that the reversible nucleation kinetics in Refs. 1 and 2 at high temperatures leads to incomplete conversion and equilibrium coexistence of the two phases, which are inconsistent with an experiment and counterintuitive.

In this note, we use our recent results on the virtual melting (VM) growth mechanism,[6–8] nucleation mechanism,[9] and some additional experiments to improve the kinetic equation and answer the above questions.

GROWTH MODEL

Two types of internal stresses may build up due to transformation strain during the PT. The first one is related to the displacement continuity across a coherent interface which will relax if the interface losses its coherence. The second one is due to a jump in volumetric transformation strain in the δ phase, if it is completely inside the β phase (even for an incoherent interface). Internal stresses should increase the PT temperature. However, since nucleation and growth of the δ phase in PBX 9501 start at the crystal surface,[9] the second type of internal stresses are absent. This is in contrast to PT in HMX crystals without the binder which starts inside the crystal.

It was found in our papers[6–8] that the energy of the internal stresses at the coherent β-δ interface is sufficient to reduce the melting temperature of the δ phase by $\sim$120 K from the thermodynamic melting temperature $\theta_m = 551$ K to $\theta_e = 432$ K (at pressure $p = 0$). After melting, the interface is incoherent and elastic energy completely disappears (that is why it reduces the melting temperature). An unstressed melt is unstable with respect to the δ phase and it solidifies into the stable δ phase. The melt in each transforming material point exists during an extremely short time, which is nonetheless sufficient for stress relaxation. It is therefore a transitional activated state rather than a thermodynamically stable melt. We called this state the VM. Reduction in volume during solidification generates tensile stresses in the solidifying layer. During solidification, the yield stress and the maximal normal tensile stress (resistance to fracture) are negligible. That is why the elastic strains completely relax through one or more of these mechanisms: vacancy generation, nanocracking, and cavitation. The characteristic size of the initial cavities is of nanometer size. However, since cracking occurs sequentially in the whole transforming volume, the size can grow by diffusion and coalescence because the temperature is high enough. This explains the nanoporosity observed experimentally in Refs. 1 and 2; without the

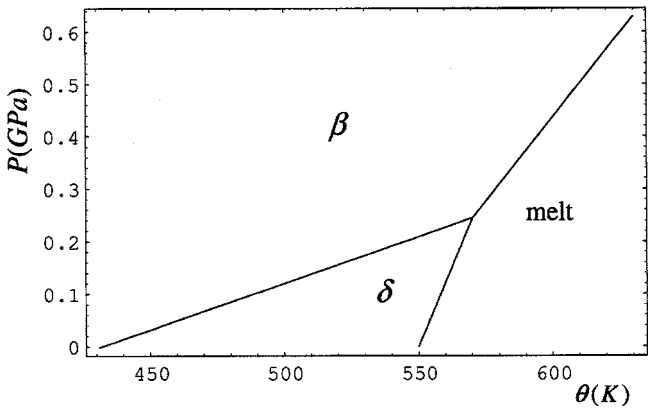

FIG. 1. Equilibrium pressure-temperature phase diagram of HMX based on Eq. (4).

VM, compressive stresses in the δ phase could not cause it. Since damage during the solidification occurs at stresses close to zero, it does not change the thermodynamics and kinetics of the $\beta \rightarrow \delta$ PT; the VM deletes the entire thermomechanical memory of preceding cycles of the direct-reverse transformation.[6–8] This explains the paradoxical independence of the thermodynamics and kinetics for the first and second $\beta \leftrightarrow \delta$ PT cycles observed in Refs. 1 and 2. Under high external pressure, we assume that porosity will be closed immediately after its appearance, because the yield stress is close to zero. Also, the athermal interface friction motion is absent for the VM mechanism because the melt as a hydrostatic medium does not interact with crystal-lattice defects.[6–8] This explains why the PT can start and progress under a small driving force. For the $\alpha \leftrightarrow \delta$ and $\alpha \leftrightarrow \beta$ PTs, volumetric strain is not sufficient for melting. This explains the large temperature hysteresis as due to elastic stresses and interface friction. The thermodynamic driving force for the $\beta \rightarrow \delta$ PT is

$$-\Delta g_{\beta\rightarrow\delta} = -(\Delta h_{\beta\rightarrow\delta} - \theta \Delta s_{\beta\rightarrow\delta}) - p\Delta v_{\beta-\delta}, \tag{1}$$

where $\Delta g_{\beta\rightarrow\delta}$, $\Delta h_{\beta\rightarrow\delta}$, $\Delta s_{\beta\rightarrow\delta}$, and $\Delta v_{\beta-\delta}$ are the change in the molar Gibbs potential, enthalphy, entropy, and volume during the $\beta \rightarrow \delta$ PT. In Ref. 1, $\Delta v_{\beta-\delta} = 1.14 \times 10^{-5}$ m^3/mole was used which corresponds to $\varepsilon^t = 0.07$; we will use $\varepsilon^t = 0.08$ (Ref. 12) and $\Delta v_{\beta-\delta} = 1.28 \times 10^{-5}$ m^3/mole. Because the change in thermal strain is small in comparison with ε^t,[3] we will neglect it. Since the maximum pressure at which the $\beta \rightarrow \delta$ PT is possible is less than 0.3 GPa (pressure at the triple point, Fig. 1) and the bulk modulus is $B = 15$ GPa, the pressure dependence of the bulk moduli can be neglected. Then the change in elastic energy is $0.5p^2[(1/B_\beta) - (1/B_\delta)]$. Since the bulk moduli have a significant scatter based on various sources[10,12] and the difference between B_δ and B_β is small, this term can be neglected in Eq. (1).

Taking $-\Delta h_{\beta\rightarrow\delta} = 9.8$ kJ/mole (Refs. 1 and 2) and $\Delta s_{\beta\rightarrow\delta} = \Delta h_{\beta\rightarrow\delta}/\theta_e = 22.68$ J/mole K we obtain

$$-\Delta g_{\beta\rightarrow\delta} = \Delta s_{\beta\rightarrow\delta}(\theta - \theta_e) - p\Delta v_{\beta-\delta}. \tag{2}$$

Similarly, the thermodynamic driving force for the melting of β and δ phases are

$$\begin{aligned} -\Delta g_{\beta\rightarrow m} &= \Delta s_{\beta\rightarrow m}(\theta - \theta_{m,\beta}) - p\Delta v_{\beta-m}, \\ -\Delta g_{\delta\rightarrow m} &= \Delta s_{\delta\rightarrow m}(\theta - \theta_{m,\delta}) - p\Delta v_{\delta-m}. \end{aligned} \tag{3}$$

Here $\theta_{m,\beta} = 532$ K and $\theta_{m,\delta} = 550$ K (Ref. 4) are the melting temperatures of the β and δ phases at ambient pressure, respectively; $\Delta s_{\delta\rightarrow m} = \Delta h_{\delta\rightarrow m}/\theta_{m,\delta} = 69900/550 = 127.09$ J/(mole K) (Refs. 1 and 2) and $\Delta s_{\beta\rightarrow m} = \Delta s_{\beta\rightarrow\delta} + \Delta s_{\delta\rightarrow m} = 149.77$ J/(mole K) are the entropy of melting of the β and δ phases, respectively; and $\Delta v_{\beta-m} = 2.33 \times 10^{-5}$ m^3/mole ($\varepsilon^t_{\beta-m} = 0.145$) and $\Delta v_{\delta-m} = \Delta v_{\beta-m} - \Delta v_{\beta-\delta} = 1.05 \times 10^{-5}$ m^3/mole ($\varepsilon^t_{\delta-m} = 0.065$) are the change in molar volume during melting of the β and δ phases.[1,2] Note that since in Ref. 1 $\Delta v_{\beta-\delta} = 1.14 \times 10^{-5}$ m^3/mole was used, it was obtained there that $\Delta v_{\delta-m} = 1.19 \times 10^{-5}$ m^3/mole.

The phase equilibrium lines for the β-δ PT and the melting of β and δ phases are obtained from the zero value of the corresponding driving force:

$$\begin{aligned} p_{\beta-\delta}(\text{MPa}) &= -765.625 + 1.772\theta, \\ p_{\beta-m}(\text{MPa}) &= -3420.600 + 6.428\theta, \\ p_{\delta-m}(\text{MPa}) &= -6657.14 + 12.104\theta. \end{aligned} \tag{4}$$

The pressure-temperature phase equilibrium diagram is shown in Fig. 1. The key point is that with growing pressure the difference in temperature between the lines of the β-δ equilibrium and the melting of β and δ phases is reduced. This makes the *VM PT mechanism easier to access at high pressures than at ambient pressure*.

NUCLEATION KINETICS

In HMX formulations with a binder, such as PBX 9501, the nitroplasticizer provides a specific mechanism for nucleation,[9] reducing the PT start temperature down to $\theta_e = 432$ K. Namely, HMX dissolves in the molten nitroplasticizer and at temperatures above θ_e nucleates the δ phase at the interface between the HMX and the binder. This mechanism is similar to the nucleation mechanism in industrial diamond synthesis under high temperature and pressure: graphite dissolves into the molten solvent metal (e.g., Fe or NiMn) and crystallizes in the form of diamond. In both cases, dissolution in and crystallization from a hydrostatic medium eliminate the nucleation barrier that is due to the energy of internal elastic stresses caused by the jump in volume during the PT. They also drastically reduce the nucleation barrier due to the change in surface energy, making nucleation possible just above the phase equilibrium temperature. The contribution of nucleation to the rate of change of the volume fraction will be described by the transition state theory,[11] in particular, by the first-order thermally activated kinetic equation:

$$\dot{c}_n = \frac{k_B\theta}{h} \exp\left[\frac{\theta S_n - H_n - p\Delta v_{\beta-\delta}}{R\theta}\right](1-c), \tag{5}$$

where k_B, h, and R are the Boltzmann, Planck, and universal

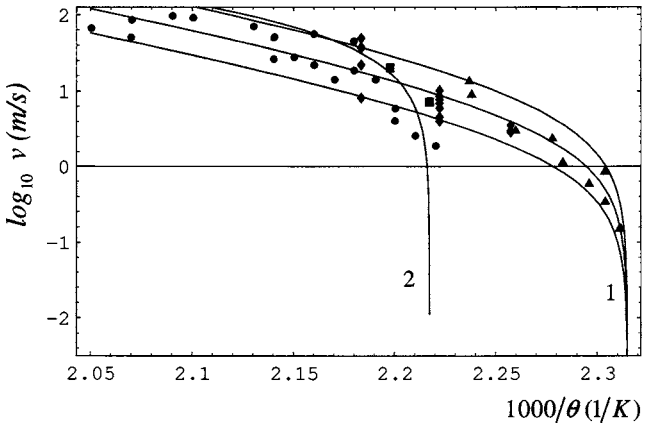

FIG. 2. A plot of the logarithm of the interface velocity ($\log v$) vs the inverse temperature ($1000/\theta$). The diamonds represent data based on our direct measurements of the interface propagation using optical movies of the visible opacity change; the rectangles are for data from similar measurements from Ref. 5; data obtained from the equation $v=l/t_{0.5}$, where $t_{0.5}$ is taken from Refs. 1 and 2 and l is the effective propagation length (chosen form the best fit), are plotted as triangles; the circles are used for experimental data from Ref. 5 obtained using DSC measurements. Line 1 is based on our Eq. (6) with three different preexponential factors, $v_0=10^4$ m/s for the middle curve; changes in the preexponential factor shift the middle curve by 0.32 up and down. Line 2 is a fit suggested in Ref. 5.

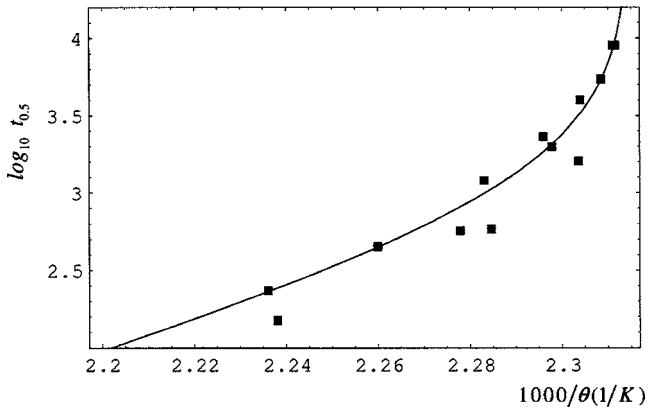

FIG. 3. A comparison of the predictions of Eq. (11) (solid line) with experimental data. The logarithm of the half-time of conversion is plotted as a function of $1000/T$ (K) for $\beta\rightarrow\delta$ PT in the HMX-based plastic-bonded explosive PBX 9501. The squares are data from measurements made by second harmonic generation (Refs. 1 and 2).

gas constants and H_n and S_n are the enthalpy and entropy of nucleation. For comparison, in Refs. 1 and 2 nucleation was considered as a reversible process which resulted in an additional term in Eq. (5). This leads to the existence of stationary values of $c<1$ for high temperatures (and pressures) when the contribution of nucleation to the overall rate greatly exceeds that of growth, which is physically contradictory. In contrast, the use of Eq. (5) leads to complete conversion.

On the other hand, in the HMX crystals without a binder, nucleation occurs at specific nucleating defects which may be inclusions of the solvent used in HMX synthesis[9] or some stress concentrators. Nucleation temperature varies in a wide range from crystal to crystal because of different potencies of nucleation cites. For example, in Ref. 5 the $\beta\rightarrow\delta$ PT was not observed below 448 K. An equation similar to Eq. (5) can be used but above the chosen nucleation temperature and with H_n and S_n determined from the best fit of experimental data.

TRANSFORMATION KINETICS

The β-δ phase interface velocity can be described by the following equation (6) based on the VM mechanism:[6]

$$\begin{aligned} v &= \bar{v}_0\left(\exp\left(-\frac{g_{\beta\rightarrow m}}{R\theta}\right)-\exp\left(-\frac{g_{\delta\rightarrow m}}{R\theta}\right)\right)\\ &= \bar{v}_0\exp\left(-\frac{g_{\delta\rightarrow m}}{R\theta}\right)\left(\exp\left(-\frac{g_{\beta\rightarrow\delta}}{R\theta}\right)-1\right)\\ &= v_0\exp\left(-\frac{\Delta h_{\delta\rightarrow m}+p\Delta v_{\delta-m}}{R\theta}\right)\\ &\quad\times\left[\exp\left(-\frac{\Delta g_{\beta\rightarrow\delta}}{R\theta}\right)-1\right], \end{aligned} \tag{6}$$

where $v_0=10^4$ m/s is the preexponential factor determined from the best fit to experiments (Fig. 2). As discussed above, athermal friction is not included. The temperature dependence of the rate constant is determined by the heat of fusion $h_{\delta\rightarrow m}$ and transformation work of fusion $p\Delta v_{\delta-m}$. Equation (6) is in a good agreement with various experiments under normal pressure (Fig. 2), including experiments from Ref. 5. The curve suggested in Ref. 5 qualitatively disagrees with experiments below 451 K. The main reason for the lower activation energy in Ref. 5 is their choice of $\theta_e=451$ K while PT proceeds even at 432.6 K.[1,2] The rate of change of concentration of the δ phase due to growth, $\dot{c}_g$, can be determined by the equation

$$\dot{c}_g=\int_\Sigma v d\Sigma/V=v_{\mathrm{av}}\Sigma/V, \tag{7}$$

where Σ is the total β-δ phase interface area and v_{av} is the interface velocity averaged over Σ. The total interface area depends on the geometry of the propagating interface. If there are numerous interfaces of stochastic geometry, then in the first approximation $\Sigma\sim c(1-c)$. This equation satisfies two limit cases that $\Sigma=0$ when $c=0$ or $c=1$. Assuming that v_{av} can be determined by Eq. (6), we obtain

$$\begin{aligned} \dot{c}_g &= Wvc(1-c)=c_o c(1-c)\exp\left(-\frac{\Delta h_{\delta\rightarrow m}+p\Delta v_{\delta-m}}{R\theta}\right)\\ &\quad\times\left[\exp\left(-\frac{\Delta g_{\beta\rightarrow\delta}}{R\theta}\right)-1\right], \end{aligned} \tag{8}$$

where W and c_0 are parameters. According to the transition state theory,[11] we assume (similar to nucleation) $c_0=Q(k_B\theta/h)$, where Q is a parameter. Then the overall nucleation and growth kinetics are described by the following equation:

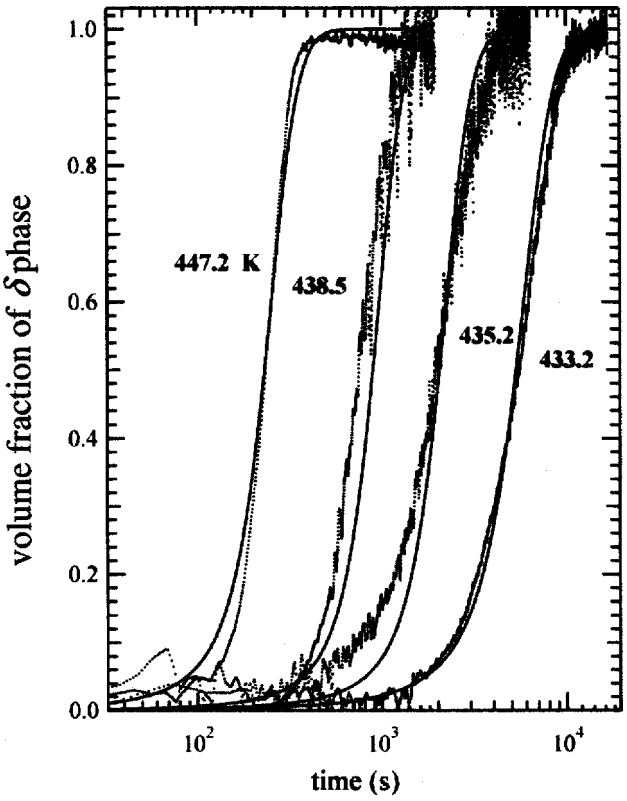

FIG. 4. A comparison of the predictions of Eq. (10) for kinetic curves $c(t)$ (solid line) with experimental data for $\beta \rightarrow \delta$ PT in the HMX-based plastic-bonded explosive PBX 9501 (Refs. 1 and 2). Isothermal measurements of the $\beta \rightarrow \delta$ PT kinetics using second harmonic generation. The data are plotted as the volume fraction of the δ phase c [equal to the square root of the measured second-harmonic generation intensity from the HMX δ phase (Refs. 1 and 2)] as a function of time t. The zero of time is the point at which the heated sample reached the labeled isothermal temperature. The solid lines are the predictions of Eq. (10).

$$\dot{c} = \dot{c}_n + \dot{c}_g = a(1-c) + bc(1-c),$$

$$a := \frac{k_B \theta}{h} \exp\left[\frac{\theta S_n - H_n - p\Delta v_{\beta-\delta}}{R\theta}\right], \tag{9}$$

$$b := Q\frac{k_B \theta}{h} \exp\left(-\frac{\Delta h_{\delta\rightarrow m} + p\Delta v_{\delta-m}}{R\theta}\right) \times\left[\exp\left(-\frac{\Delta g_{\beta\rightarrow\delta}}{R\theta}\right) - 1\right].$$

The three parameters in Eqs. (9), $H_n = 309.328$ kJ/mole, $S_n = 374.239$ J/mole K, and $Q = 7 \times 10^{-13}$, were determined from the best fit of experimental data on the time to complete half of the transformation for $\beta \rightarrow \delta$ PT.[1,2] The analytical solution to the differential Eq. (9) for fixed a and b and initial condition $c(0) = 0$ is as follows:

$$c = \frac{a(e^{(a+b)t} - 1)}{b + ae^{(a+b)t}}. \tag{10}$$

From the condition $c = 0.5$ one can find the time to half-conversion which was used in Refs. 1 and 2 to compare with experiment. We obtained

$$t_{0.5} = \frac{\ln(2 + (b/a))}{b + a}. \tag{11}$$

In Fig. 3, comparison of the prediction of Eq. (11) with the experimental data on time to half-conversion for $\beta \rightarrow \delta$ PT (Refs. 1 and 2) demonstrates good agreement. The individual $c(t)$ curves in the temperature range 433.2–447.2 K are in good correspondence with experiment[2] as well (Fig. 4).

In summary, we further developed the thermodynamic and kinetic models presented in Refs. 1 and 2, especially in the direction of better justification.

ACKNOWLEDGMENTS

One of the authors (V.I.L.) acknowledges the support of NSF (CMS-02011108) and LANL (13720-001-05-AH). The other authors (B.F.H., L.B.S., and B.W.A.) acknowledge the support of the Laboratory Research and Development and H.E. Science Programs at Los Alamos National Laboratory.

[a] Electronic mail: valery.levitas@ttu.edu

[1] B. F. Henson, L. B. Smilowitz, B. W. Asay, and P. M. Dickson, J. Chem. Phys. **117**, 3780 (2002).
[2] L. B. Smilowitz, B. F. Henson, B. W. Asay, and P. M. Dickson, J. Chem. Phys. **117**, 3789 (2002).
[3] M. Herrmann, W. Engel, and N. Eisenreich, Propellants, Explos., Pyrotech. **17**, 190 (1992).
[4] H. H. Cady, 17th International Annual Conference of the Institut Chemische Technologie, Karlsruhe, FRG, 1986, pp. 17.1–17.12.
[5] A. K. Burnham, R. K. Weese, and B. L. Weeks, J. Phys. Chem. B **108**, 19432 (2004).
[6] V. I. Levitas, B. F. Henson, L. B. Smilowitz, and B. W. Asay, Phys. Rev. Lett. **92**, 235702 (2004).
[7] V. I. Levitas, L. B. Smilowitz, B. F. Henson, and B. W. Asay, Appl. Phys. Lett. **87**, 191907 (2005).
[8] V. I. Levitas, L. B. Smilowitz, B. F. Henson, and B. W. Asay, Phys. Rev. B (submitted).
[9] L. B. Smilowitz, B. F. Henson, M. Greenfield, A. Sas, B. W. Asay, and P. M. Dickson, J. Chem. Phys. **121**, 5550 (2004).
[10] R. Menikoff and T. D. Sewell, Combust. Theory Modell. **6**, 103 (2002).
[11] T. D. Sewell, R. Menikoff, D. Bedrov, and G. D. Smith, J. Chem. Phys. **119**, 7417 (2003).
[12] G. G. Hammes, *Principles of Chemical Kinetics* (Academic, New York, 1978).